RESEARCH ARTICLE

A New Alarm System Developing Approach Through Graph Modeling

KOUROSH PARSA[1], (Senior Member, IEEE), **MAUREEN HASSALL**[2],
MOHSEN NADERPOUR[3], **MOBIN POURREZA**[4], AND **FAHIMEH RAMEZANI**[3]

[1]School of Information Technology and Electrical Engineering (ITEE), The University of Queensland, Brisbane, QLD 4072, Australia
[2]Sustainable Minerals Institute, The University of Queensland, Brisbane, QLD 4072, Australia
[3]Australian Artificial Intelligence Institute (AAII), University of Technology Sydney (UTS), Sydney, NSW 2007, Australia
[4]Fachhochschule Dortmund, 44139 Dortmund, Germany

Corresponding author: Mohsen Naderpour (Mohsen.Naderpour@uts.edu.au)

ABSTRACT The alarm system is an overarching component in effectively managing abnormal situations. To enhance its efficacy, we have previously developed an alarm graph modelling (AGM) that overcomes the challenges of traditional methods in alarm workshops. This paper develops an integrated platform that is used for the justification and verification of AGM and other theoretical purposes in the future. Despite the limited availability of process simulations, we successfully updated the Tennessee Eastman Process Simulink model to work seamlessly with the alarm system. The outcomes of the alarm workshop were then implemented, and the alarms were adjusted accordingly. By analyzing predefined scenarios, we were able to evaluate the AGM's ability to accurately represent abnormal event progression, thereby validating and fine-tuning the alarm system.

INDEX TERMS Alarm modelling, alarm tuning, Tennessee Eastman process, safety-critical systems, graph modelling and theory.

I. INTRODUCTION

A properly configured alarm system serves the crucial purpose of notifying operators of any anomalous occurrences. However, incorrect configuration may lead to problems such as nuisance alarms and alarm floods, significantly diminishing their effectiveness [1]. This is especially the case for process controls that play a crucial role in process operation and cannot be replaced by any other engineering discipline. Nevertheless, it is often overlooked and not given the recognition it deserves in plant operation [2]. To control the abnormal events in operation, process variables are used to define the alarms and trip when the value exceeds certain limits, and then the alarm or trip will be activated [3]. A false alarm that is incorrectly activated within normal operation or a missed alarm that failed to be activated when it should be may reduce the alarm system's reliability [4]. Dead-bands and predetermined delays are the conventional approaches

The associate editor coordinating the review of this manuscript and approving it for publication was Lorenzo Ciani.

to reducing false alarms and missed alarms [5]. To prevent overwhelming the operator or compromising the safety of the operation, it is important to use the appropriate number of alarms, and it is crucial to ensure that the number of alarms is justified [6]. Alarm issues, such as chattering, nuisance alarms, and alarm floods, severely impact the efficiency of alarm management, which could lead to a trip [7]. Accurate setting of alarm setpoints and performance of the alarm system are crucial in reducing operator workload and improving alarm performance. Alarm overload primarily stems from chattering alarms, accounting for 70% of all alarm issues [8]. Process operators often set alarm thresholds arbitrarily and excessively, leading to a high number of process alarms. These poorly configured limits can result in redundant and chattering alarms, as well as long-standing alarms. In critical situations, an overwhelming flood of alarms can hinder or completely prevent operators from identifying the root cause [9], [10].

Our previous studies developed an innovative alarm graph modelling called AGM, detailed by Kourosh et al. in [3],

[6], and [11], that relies on graph theory's capabilities and seizes traditional techniques' limitations. In continuing, this paper develops an integrated platform based on the Tennessee Eastman Process (TEP) Simulink model to verify and evaluate the efficiency of the AGM. The Tennessee Eastman Process, initially crafted by Downs and Vogel in 1993 [12], is a vital resource in system theory for comparative studies and algorithm validation. It has been employed for fault diagnosis by Yin et al. [13] and system identification by Bathelt et al. [14]. The model is founded on an authentic process, yielding a non-linear model of a multifaceted multicomponent system, which makes it a well-known model in academic studies as an open-source simulation. Given the model's widespread employment, it is paramount that its code is executed impeccably. TEP simulation serves to evaluate the effects of distinct process variables, such as control valves, feeding rate, agitator speed rate, and disturbances on the production rate and G component percentage in production [15], [16]. All the process variables in this simulation are controlled through the proportional integrator differentiator (PID) controllers, which was the primary intention of the simulation developers Ricker [17]. The TEP simulation code was created using non-linear programming for real-time use, which includes the C-mex platform for formulation and dynamic optimization. As part of this study, an alarm system was designed and added to TEP based on data from Kourosh et al. [11] that is included in the alarm system for conducting experiments. This approach enables better calibration of alarms and detection of successive abnormal events, even those that lead to plant shutdowns. Likewise, this method is beneficial because the results are not significantly affected by the number of alarms, how quickly they spread, how long the situation lasts, or the time between events.

The rest of this paper is organized as follows: Section II details the alarm system's development on the TEP simulation platform, the GUI's development, and finally, the alarm tuning. Section III is designed to run trials based on typical abnormal scenarios, such as high and unstable feeding, no feed, and loss of cooling water flow, to test the alarm system's robustness and verify its ability to capture an abnormal event through the AGM. Finally, Section IV summarises the achievements and discusses future works and limitations.

II. ALARM SYSTEM IMPLEMENTATION
In this section, the TEP is employed to demonstrate the performance of the AGM and evaluate the alarm system. TEP was created to benchmark a simulated industrial process to evaluate process control and monitoring techniques [14]. TEP dynamic is programmed in C-mex, and all plant control and safety systems are installed in the MATLAB/Simulink environment [14]. In order to ensure an effective alarm system, it is crucial that the simulation architecture closely mirrors the actual plant control system. By doing so, this research will be able to conduct trials that accurately simulate
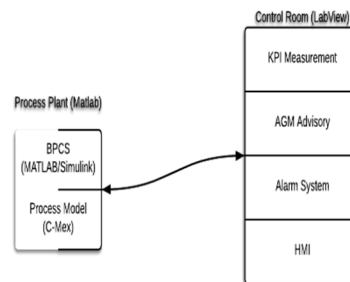

FIGURE 1. Configuration of the alarm system.

real-life scenarios. In this architecture, all supervisory data is communicated through the serial Modbus protocol to the LabView environment, which includes the HMI. Figure 1 illustrates the system architecture.

The P&ID as shown in Figure 2, displays the designed alarms, and Table 1 presents the corresponding abstracted alarm database. In the TEP alarm system, alarms are created for each data stream associated with a particular process variable based on the original model [14]. For example, xmeas42 represents the A feed flow temperature.

Connecting the process simulation from Simulink/MATLAB to the supervisory control and alarm system in LabView is challenging due to the multilayer structure of the simulation and the real-time communication between the two programming environments [14]. However, various techniques have been explored to exchange data between LabVIEW and Simulink environments to enable communication between the parts of the OTS. NI LabVIEW has developed interfacing methods to communicate with MATLAB and Simulink models, which have been refined with each version of the LabVIEW software [18]. Despite the three-step process of developing interface modules, compiling, and updating the code, the journey to communicate the TEP Simulink to the alarm system in the LabVIEW environment.

A. SIMULINK AND LABVIEW INTERFACING
To establish communication between two computers using hardware ports, Simulink and LabView functions are used for serial and Ethernet transmission. If two computers do not have two Ethernet cards, an Ethernet card and a USB-Ethernet adapter can be used, or a serial-to-Ethernet converter can be adapted and configured. However, synchronization during data transfer can cause instability in the communication channel, and noise on the ports can sometimes cause data malfunction. To address these issues, a solution was incorporated using serial COM ports and virtual pairing of ports without a converter or physical medium. This reduces noise and allows each program to use one of the paired comports for data transfer [19]. The interface development configuration for serial COM port interfacing is presented in Figure 3. Figure 4 shows the part of the programming has been developed to send and receive data via serial COM ports.

TABLE 1. Abstracted alarm database.

| No	Data stream	Alarm Tag	Alarm Control Function	Normal Operation	Alarm Setpoint	Corrective Action	Consequence severity
1	xmeas42	TAH-01	Temperature on Feed A	45°C	50°C	Reduce feed A flow	Minor
		TAL-02			40°C	N/A	Minor
2	xmeas43	TAH-03	Temperature on Feed D	45°C	50°C	Reduce feed D flow	Minor
		TAL-04			40°C	N/A	Minor
3	xmeas44	TAH-05	Temperature on Feed E	45°C	50°C	Reduce feed E flow	Minor
		TAL-06			40°C	N/A	Minor
4	xmeas45	TAH-07	Temperature on Feed C	45°C	50°C	Reduce feed E flow	Minor
		TAL-08			40°C	N/A	Minor
5	xmeas9	TAHH-11	Temperature on Reactor	120.4°C	130°C	Increase CW flow	Major
		TAH-09			125°C	Decrease the agitator rate	Medium
		TAL-10			115°C	Increase the agitator speed	Low
		TALL-12			110°C	Decrease CW flow	Medium
6	xmeas21	TAH-13	Temperature on inlet /outlet CWS -Reactor	35°C	45°C	Decrease the reactor feed	Medium
		TAL-14			25°C	Decrease CW flow	Minor
		TAH-15		94.6°C	103°C	Decrease the reactor feed	Medium
		TAL-16			85°C	Reduce cooling water flow	Minor
7	xmeas48	TAH-17	Temperature on CWS inlet Separator	40°C	45°C	Increase CW flow	Medium
		TAHH-18			50°C	Increase CW flow	Major
8	xmeas22	TAH-19	Temperature Conden CWR	77.3°C	95°C	Increase CW flow	Minor
		TAL-20			80°C	Decrease CW flow	
9	xmeas11	TAH-21	Temperature on Separator	80.2°C	90°C	Increase discharge from separator	Minor
		TAHH-22			100°C	Increase discharge to reactor	High
10	xmeas18	TAHH-25	Temperature on Stripper	65.7°C	75°C	Stop the boiler	High
		TAH-23			68°C	Discharge to reactor	Medium
		TAL-24			64°C	Increase feeding to Stripper	Low
		TALL-26			50°C	Increase Boiler Temperature	Medium
11	xmeas8	LAH-01	Level Alarm on Reactor	75%	80%	Stop feeding to Reactor	Medium
		LAHH-03			85%	Stop feeding to Reactor	High
		LAL-02			60%	Increase feeding	Low
		LALL-04			50%	Increase feeding /Trip	Medium
12	xmeas12	LAH-09	Level Alarm on Separator	50%	60%	Discharge to Stripper	Medium
		LAHH-11			65%	Discharge to Stripper	High
		LAL-10			40%	Stop discharge pump	Low
		LALL-12			35%	Stop discharge pump	High
13	xmeas15	LAH-13	Level Alarm on Stripper	50%	60%	Stop pump in from separator	Medium
		LAHH-15			70%	Discharge product	High
		LAL-14			35%	Stop product pump	Low
		LALL-16			25%	Stop boiler	High
14	xmeas1	FAH-01	Flow Alarm on Feed A	0.25052 kscmh	0.5kscmh	Reduce feed A flow	Low
		FAL-02			0.1kscmh	Increase feed A flow	Low
15	xmeas2	FAH-03	Flow Alarm on Feed D	3664 kg/h	3680kg/h	Reduce feed D flow	Low
		FAL-04			3650kg/h	Increase feed D flow	Low
16	xmeas3	FAH-05	Flow Alarm on Feed E	4509.3 kg/h	4530kg/h	Reduce feed E flow	Low
		FAL-06			4490kg/h	Increase feed E flow	Low
17	xmeas4	FAH-07	Flow Alarm on Feed C	9.3477 kscmh	9.5kscmh	Reduce feed C flow	Low
		FAL-08			9.2kscmh	Increase feed C flow	Low
18	xmeas6	FAH-09	Flow Alarm on Reactor	42.339 kscmh	42.7kscmh	Reduce feed flows A, D and E	Low
		FAL-10			42kscmh	Increase feed flows A, D and E	Low
19	xmeas47	FAH-11	Alarm on Reactor CWS	93.37 m3/h	100m3/h	Reduce CW flow	Low
		FAL-12			85m3/h	Increase CW flow	Low
20	xmeas49	FAH-13	Condenser CWS	49.37 m3/h	60m3/h	Reduce CW flow	Low
		FAL-14			40m3/h	Increase CW flow	Low
21	xmeas5	FAH-15	recycle line from Sep-Re	26.902 kscmh	28 kscmh	Reduce recycle flow	Low
		FAL-16			26 kscmh	Increase recycle flow	Low
22	xmeas14	FAH-17	Separator to Stripper	25.160 m3/h	27 m3/h	Reduce flow from Separator	Low
		FAL-18			24 m3/h	Increase flow from Separator	Low
23	xmeas17	FAH-23	Flow on Product line	22.949 m3/h	27 m3/h	Reduce flow via control valve	Low
		FAL-24			20 m3/h	Increase flow via control valve	Low
24	xmeas10	FAH-21	High Flow on purge rate	0.33712 kscmh	0.6kscmh	Increase compression to the Reactor	Low
		FAHH-22			0.7kscmh	Trip the plant	Low
25	xmeas19	FAH-25	Flow on Stripper steam flow	230.31kg/h	240kg/h	Reduce flow	Low
		FAHH-26			250kg/h	Increase flow	Low
26	xmeas7	PAH-01	Pressure Alarm on Reactor	2705 kPag	2810kPag	Increase CW-flow, Stop Agitator	Medium
		PAHH-02			2770kPag	Increase CW-flow, Plant Trip	High
27	xmeas13	PAH-05	Pressure on Separator	2633.7 kPag	2710kPag	Increase compression to the Reactor, Increase purge flow via CV -1005	Medium
					2720kPag	Increase purge flow via CV -1005, Trip the plant	High
28	xmeas16	PAH-07	Pressure on Stripper	3102.2 kPag	3340kPag	Reduce Steam flow	Medium
		PAHH-08			3360kPag	Reduce flow in via CV-1301 and CV-1004, Trip the plant	High
29	xmeas20	CPF-01	Compressor Failure	341.43 kW	350kW	Increase Condenser CW-flow increase discharge separator	Medium
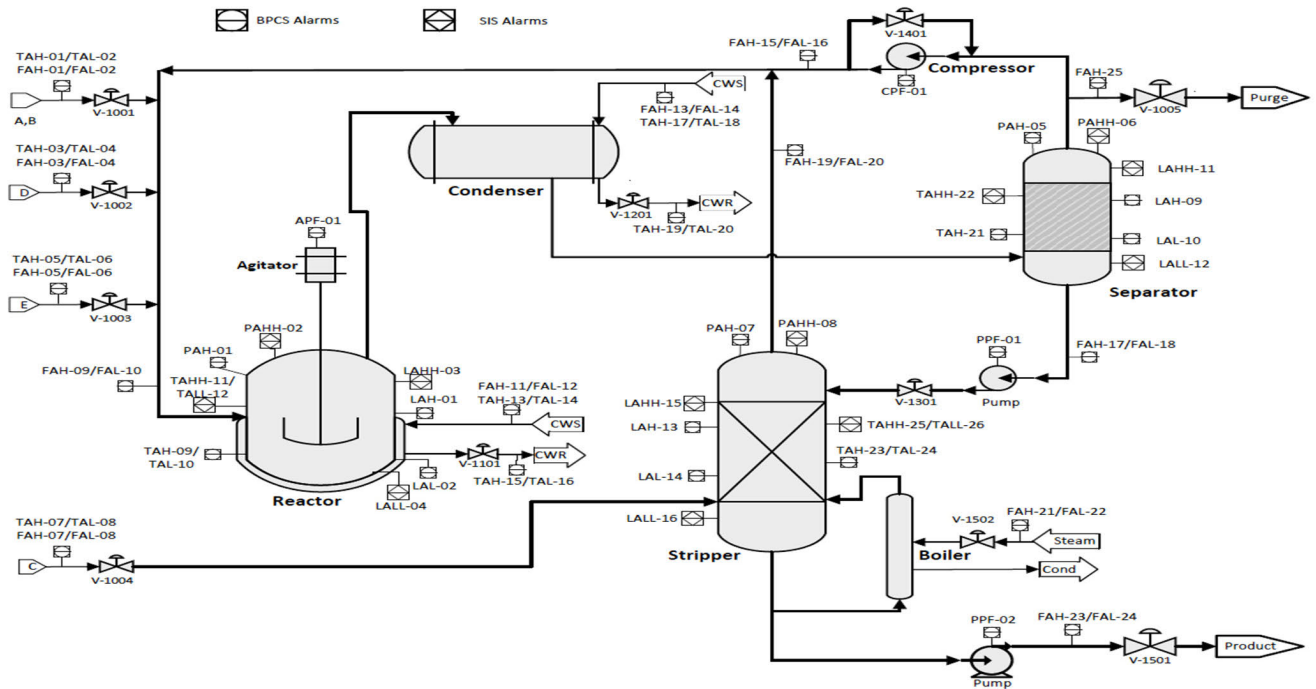
FIGURE 2. TEP updated P&ID.
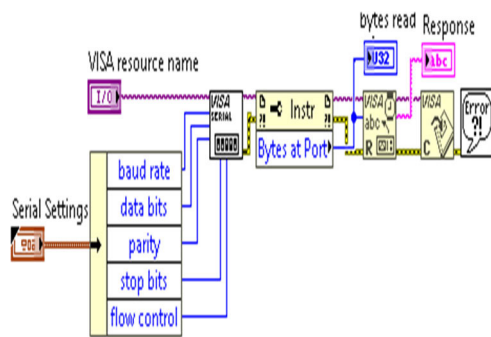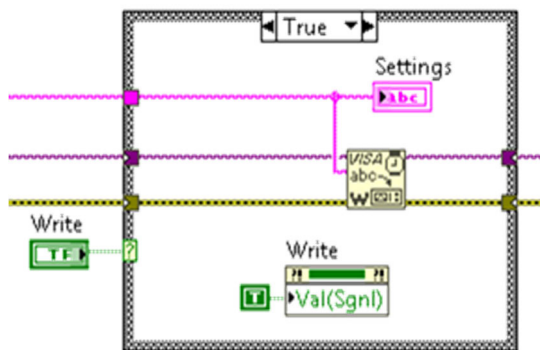

FIGURE 3. Serial send block arrangement.

FIGURE 4. Writing data in LabView.

As can be seen from Figure 3, the common method used to read a COM port is First, the COM port settings such as baud rate, data bits, parity, stop bit, and flow control must be
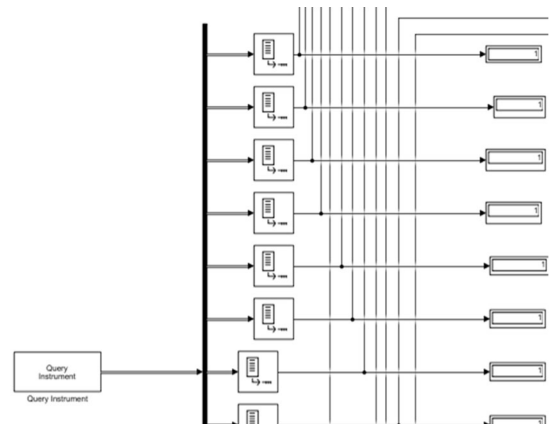

FIGURE 5. Serial receive block in MATLAB.

defined using the 'Configure Port block'. This step requires the definition of a comport name. The 'Visa Read block' is used to read input data, and the number of received bytes must be specified, as shown in Figures 3 and 4. To avoid data collision and ensure real-time control, control and monitoring must be performed simultaneously when transferring data to the COM port. Using a loop structure for receiving data and a case structure for updates can improve results. The 'Query instrument block' in MATLAB/Simulink can capture receiving data, but COM port settings must match those of LabView as shown in Figures 5 and 6. Indeed, the buffer solution prevents data overflow.

After configuring the COM ports in Simulink and Lab-VIEW, defining the data format was critical to data exchange.
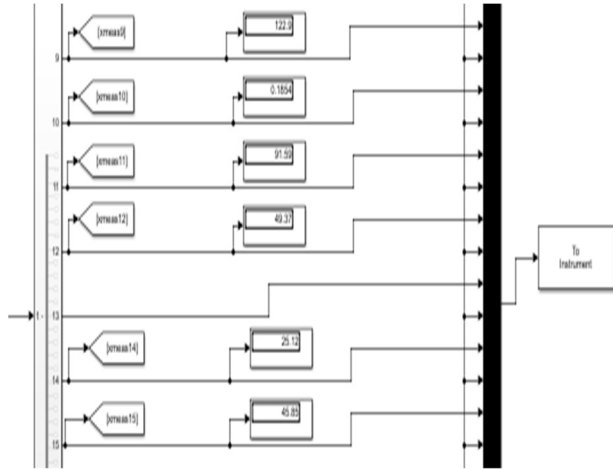
FIGURE 6. Serial sending block in MATLAB.

LabView Serial Visa blocks generally work with ASCII format; consequently, the data transmission format is set to ASCII, and the conversion program is added to the Simulink program, as shown in Figure 7.

B. DATA COMMUNICATION COMMANDS
Table 2 shows the addresses for data streams sent to Lab-VIEW using Modbus serial. the communication between Simulink and LabVIEW can be monitored through HSI as detailed in Table 2. If there are issues, the communication speed can be adjusted to fix address synchronization problems.

Our approach for integrating operator responses into Simulink's process simulation through the alarm system interface avoids changes to controller parameters or variable overrides. Instead, we use coefficients to transfer data to the simulation's core component. This ensures high integrity by including C-mex code, PID loop controllers, and communication blocks.

C. TEP ALARM DISPLAY
The process display follows industry best practices and adheres to standards recommended by ISA-101 [20]. It resembles the familiar P&ID format and uses a recommended grey code, with red only for alarm activations. It is designed for a 32″ wide display, and the alarm system is organized into 5 tabular pages.

Tab-1 shows the P&ID with all the alarms and valve control commands, as shown in Figure 8.1. Tab-2 shows the devised AGM to illustrate how alarms are activated and progress if not managed, as shown in Figure 8.2. Figure 8.3 shows Tab-3 in which the communication setting between LabView and Simulink, including all the channel settings and data transfer checking can be either reviewed or modified.

Also, the address the trial data will be saved can be selected from this page. Tab-4 shows the real-time monitoring of the process variable data stream to understand the process and
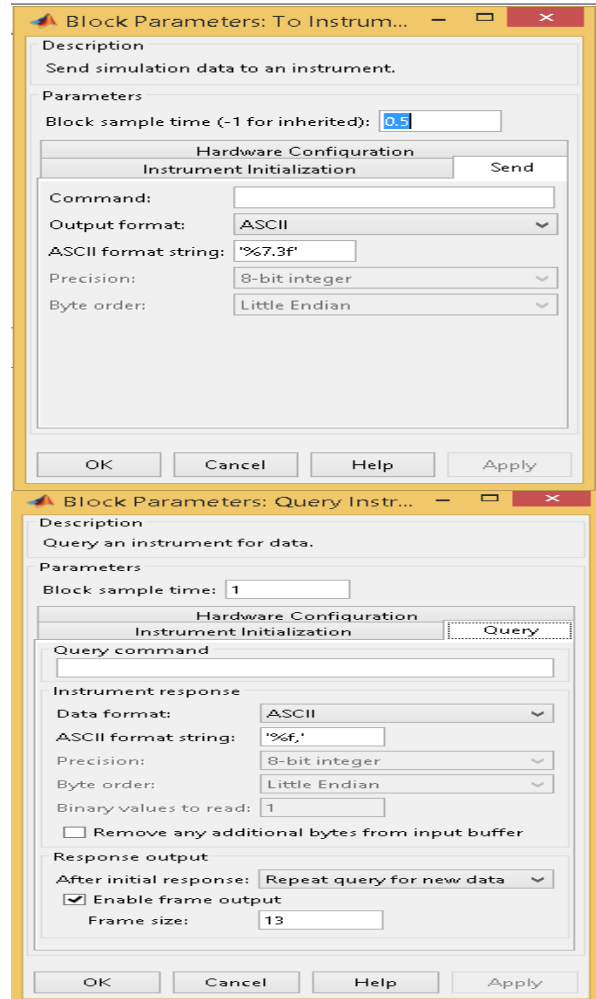

FIGURE 7. Data format setting in MATLAB.

real-time supervisory control, as shown in Figure 8.4. Tab-5 shows the alarm setpoint where all the alarm settings can be defined and tuned for the operation; all the alarms can be reset to the initialized value after each run with the reset key, as shown in Figure 8.5.

D. ALARM TUNING
After careful study and a couple of iterations of running the TEP simulation process, the alarm system setpoints are revised to reduce alarm hysteresis and standing according to the EEMUA and ISA-18, as shown in Table 3. Furthermore, the statistical analysis, e.g., maximum 10%, minimum 10% average quantity, has been carried out to update the alarm setpoints. The current status of the alarm tuning process towards the final values can be found in Table 3. Any revised items are highlighted in red for easy identification.
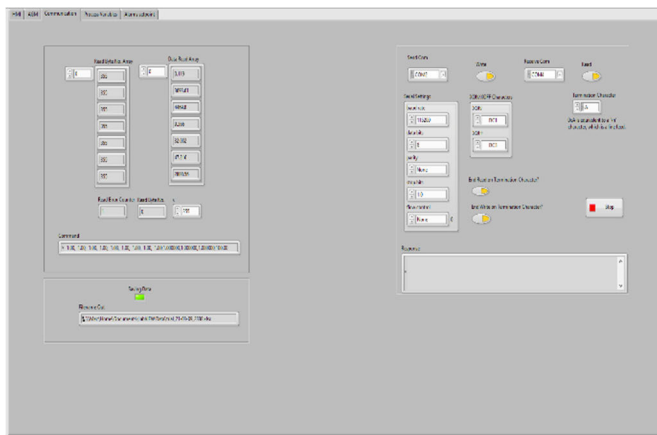
The TEP model process simulation has been extensively studied to develop a controller that maintains the process variables within the normal operating range. The controller's parameters have been carefully tuned to ensure that the entire control system is highly resistant to disturbances, making it
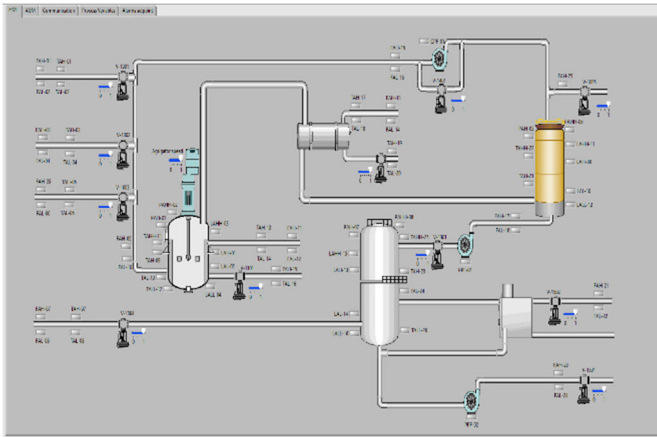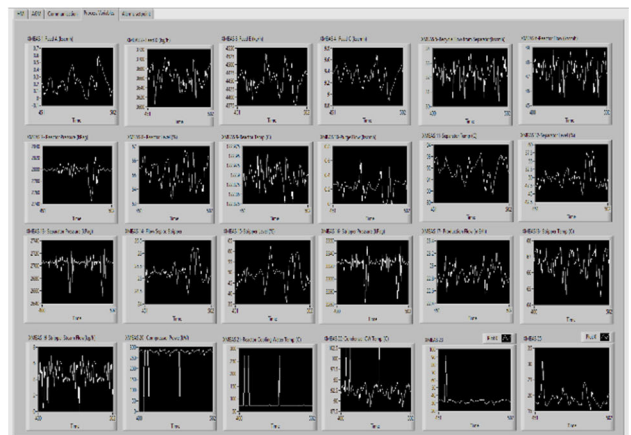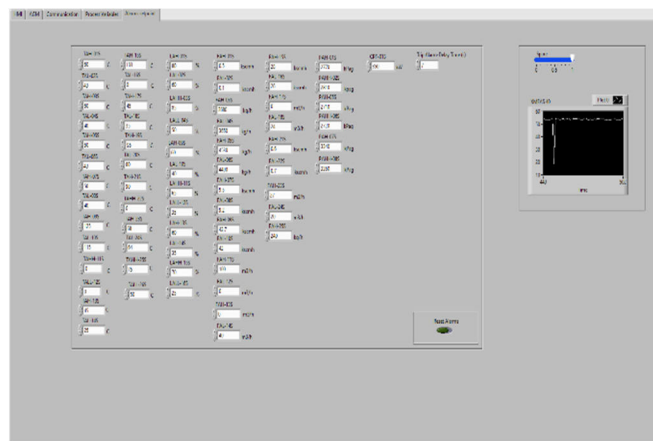
(1) TEP Process Control Interface
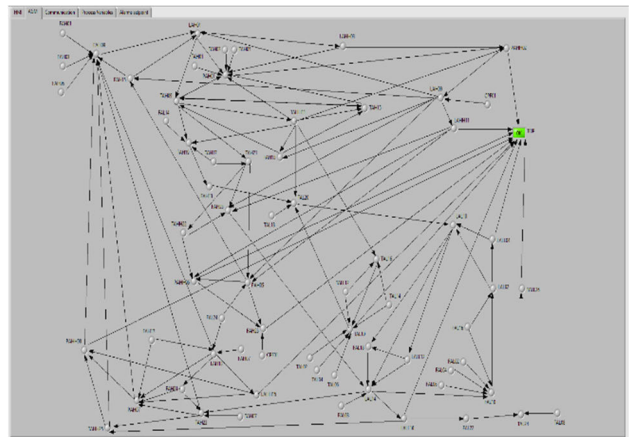
(2) Alarm Graph Model

(3)TEP Process Control Interface

(4)TEP Process Control Interface

(5) TEP Process Control Interface

FIGURE 8. TEP HMI.

challenging to destabilize the TEP. Multiple scenarios have been planned to verify and validate the proposed AGM. Verification scenarios will test the alarm system's capacity and evaluate the alarm activation sequence.

III. VERIFICATION EXPERIMENTS

During the verification process, we intentionally destabilized the process control and allowed failures to occur without responding to alarms. These experiments aim to test the

TABLE 2. Abstracted alarm database.

xmeas	Description	Unit	Comm Address
xmeas-1	A Feed	kscmh	1
xmeas-2	D Feed	kg/hr	2
xmeas-3	E Feed	kg/hr	3
xmeas-4	A and C Feed	kscmh	4
xmeas-5	Recycle Flow'	kscmh	5
xmeas-6	Reactor Feed Rate	kscmh	6
xmeas-7	Reactor Pressure	kPag	7
xmeas-8	Reactor Level	%	8
xmeas-9	Reactor Temperature	Deg C	9
xmeas-10	Purge Rate	kscmh	10
xmeas-11	Product Sep Temp	Deg C	11
xmeas-12	Product Sep Level	%	12
xmeas-13	Product Sep Pressure	kPa gauge	13
xmeas-14	Product Sep Underflow	m3/hr	14
xmeas-15	Stripper Level	%	15
xmeas-16	Stripper Pressure	kPa gauge	16
xmeas-17	Stripper Underflow	m3/hr	17
xmeas-18	Stripper Temp	Deg C	18
xmeas-19	Stripper Steam Flow	kg/h	19
xmeas-20	Compressor Work	kW	20
xmeas-21	Reactor Coolant Temp	Deg C	21
xmeas-22	Separator Coolant Temp	Deg C	22

TABLE 3. TEP alarms system setpoints.

Alarm	FAH-01	FAL-02	FAH-03	FAL-04	FAH-05	FAL-06	FAH-07	FAL-08	FAH-09	FAL-10
	0.5	~~0.1~~ 0.05	3680	~~3650~~ 3620	~~4520~~ ~~4650~~ 4490	~~4200~~ 4396	~~9.5~~ 9.4	~~8.7~~ 9	~~46~~ 48.5	~~42~~ 41

Alarm	FAH-15	FAL-16	FAH-17	FAL-18	FAH-21	FAL-22	FAH-23	FAL-24	FAH-25	PAH-01
	~~34~~ 33.3	~~36~~ 33.3	~~38~~ 25.9	~~24~~ 25	~~0.6~~ 6.15	~~0.7~~ 3.14	~~37~~ 30	~~30~~ 10	~~340~~ 0.42	~~2810~~ 2807

Alarm	PAHH-02	PAH-05	PAHH-06	PAH-07	PAHH-08	CPF-01	TAH-09	TAL-10	TAHH-11	TALL-12
	~~3820~~ 2812	~~2710~~ 2707	~~2720~~ 2712	~~3340~~ 3337	~~3360~~ 3340	~~340~~ 295	~~136~~ 122.89	~~145~~ 122.8	~~130~~ 123	~~140~~ 121

Alarm	TAH-13	TAL-14	TAH-15	TAL-16	TAH-19	TAL-20	TAH-21	TAHH-22	TAH-23	TAL-24
	~~87~~ 75	~~75~~ 70	~~105~~ 73	~~85~~ 72	95	~~90~~ 87	~~95~~ 92.9	~~105~~ 94	~~65~~ 67.4	~~66~~ 65.3

Alarm	TAHH-25	TALL-26	LAH-01	LAL-02	LAHH-03	LALL-04	LAH-09	LAL-10	LAHH-11	LALL-12
	~~75~~ 67.8	~~55~~ 64.5	~~60~~ 65.7	~~50~~ 63.6	~~60~~ 67	~~50~~ 61	~~60~~ 55	~~50~~ 47	~~62~~ 56.5	~~35~~ 42

Alarm	LAH-13	LAL-14	LAHH-15	LALL-16	TAH-17	TAL-18				
	~~60~~ 58	~~35~~ 42	~~70~~ 62	~~25~~ 38	94	80				

alarm activation sequence and adjust alarms as needed by manipulating the process to create instability.

A. MANIPULATED PID CONTROLLERS
We intentionally overfilled equipment and monitored alarms until the trip alarm was triggered by manipulated feed flow PIDs and introducing destabilizing valve controllers, as addressed in Table 4.

The operation stopped unexpectedly after running for 56.59 hours instead of the planned duration. Following is

TABLE 4. Manipulated PID controllers.

Changing P Parameter	Original Kc	Manipulated Kc
A Feed	0.01	1
D Feed	1.06E-06	1
E Feed	1.80E-06	1
A&C Feed	0.003	1

an analysis of the process variables during this situation. As can be seen, manipulating the proportional value of the PIDs related to the A and A+C feed controllers (Figure 9), and D & E feed controllers (Figure 10) made the feed flow completely unstable, which mainly caused the operation trip. Figures 11 and 12 show costs, quality, production levels, and active alarms. Costs varied greatly, but quality and production were maintained. The highest number of alarms occurred around the trip time, with an alarm flood condition when the anomaly triggered. The review of the experiment aims to examine the correlation between the AGM and the abnormal situation progression. Through scenario analysis, it was found that there were consistently more than ten alarms (with a maximum of 14 alarms) between 40.13 and 54.53 hours, which led to trips due to a lack of response to the alarms.
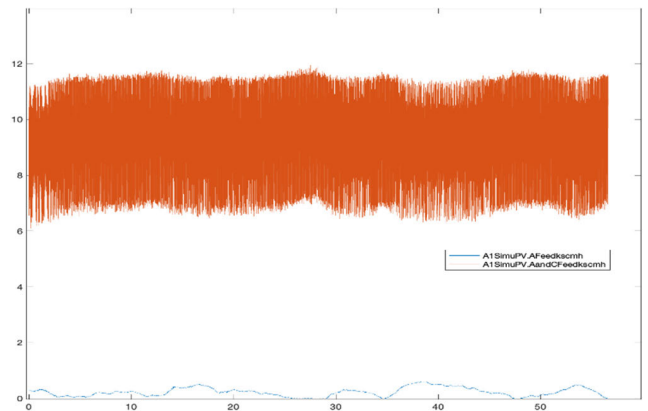
FIGURE 9. A, A&C feed flow (kscmh per hour).

Among all the APTTs. The first path explains the active alarms, which are related to the low stripper level while the boiler is in operation. The alarms and trips are designed to protect the equipment from damage caused by a low-low level.

- FAL-08, FAL-18 -> LAL-14 -> LALL-16 -> Trip.
  This trip path activated in this scenario is related to the stripper's low level and may cause damage to the equipment and catalyst. In this APTT, constant low feed into the stripper triggered the low and then low-low level alarm activated, and while the boiler is working, the operation may damage either catalyst or equipment.
- TAH-21 -> PAH-05 -> PAHH-06 -> FAH-25 -> Trip.
  This ATTP shows the activated alarms related to the high temperature and pressure at the Separator, which ended in the increased release and consequently tripped. As can be
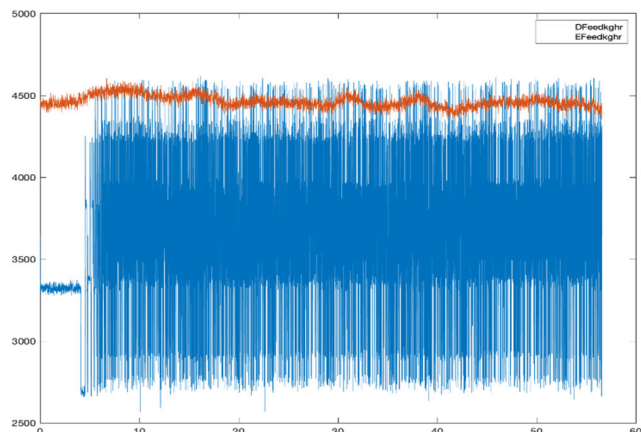
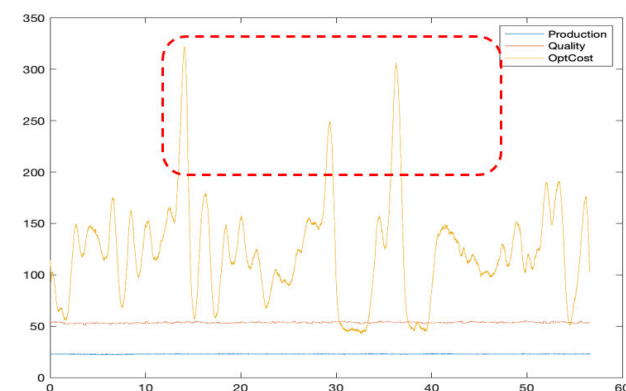**FIGURE 10.** D and E feed flow (kg/hr).
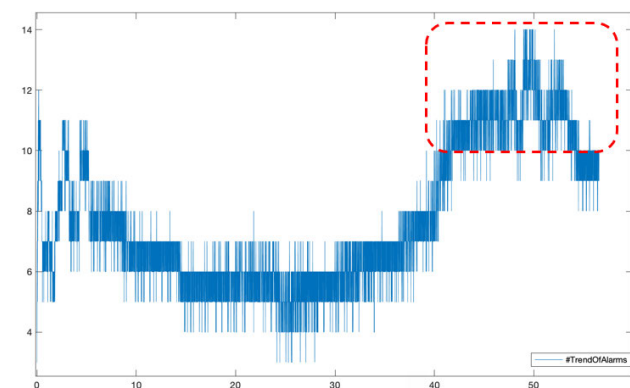

FIGURE 11. Operation cost, quality and production.

FIGURE 12. Trend of active alarms (Qty vs hours).

FIGURE 13. Reactor pressure (kPag vs hours).
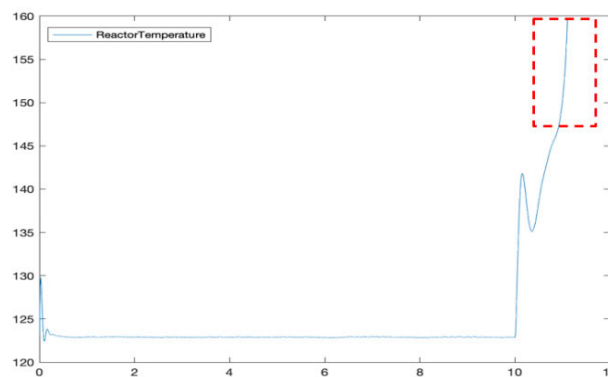
FIGURE 14. Reactor temperature (°C vs hours).

seen, the AGM can trace the chain of abnormal events and their progression to the trip for the actual causes, which was the purpose of the verification at this stage. In the next experiment, another scenario is designed to see if the AGM can trace the alarm progression and chain of the abnormal event once the cooling water system is interrupted.

B. INTERRUPTING THE COOLING WATER SYSTEM
During this experiment, using the related controller, the cooling water system was intentionally reduced to 45% of its normal rate at the 10th hour of operation. The goal was to observe the activation of the high-temperature and high-pressure failure pathways. This test helps verify the AGM failure pattern, fine-tune the alarms, and confirm the performance of the alarm system. This scenario tripped after 11.1:04, compared to the normal 100 hours of operation. Figures 13 and 14 show that the reactor process variables, reactor level started to reduce due to lack of cooling water flow, although the pressure and temperature surged, as highlighted in the red boxes, and it was one of the factors which contributed to the trip or high purge consequently. A high purge rate is another process factor contributing to the failure, as shown in Figure 15. Figure 16 shows how reducing the coolant flow increased the coolant temperature, which caused it to trip. Figure 17 shows the trend of active alarms, indicating that the number of active alarms before the 10th hour of operation was in the manageable range of under ten alarms per minute. However, the maximum number of alarms was 12 around 2.5 hours after the process started for a short period; on average, around four alarms per minute were active. But after triggering the scenario, the number of active alarms started to surge and picked at 27 alarms at 11 hours of operation.

A review of the AGM (Figure 18) against this abnormal scenario led to addressing the below APTTs as an ongoing
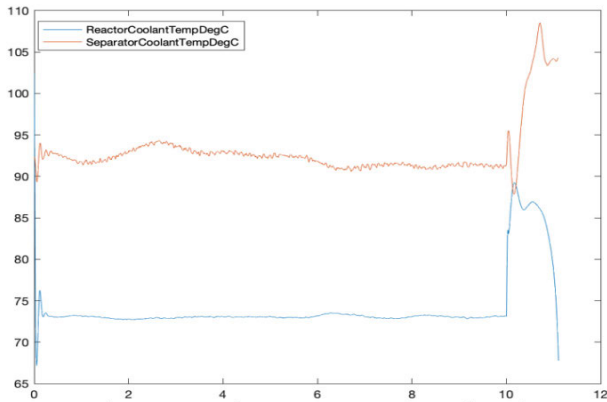
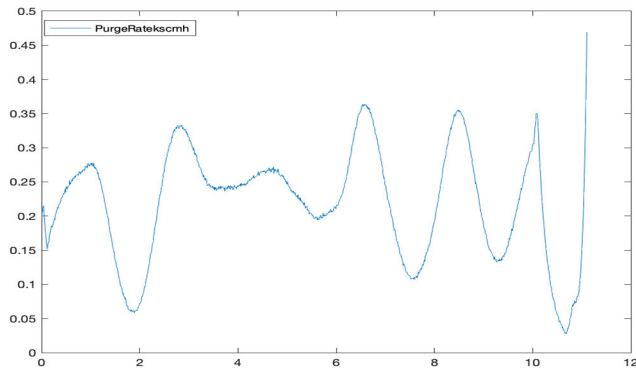**FIGURE 15.** Coolant temperature (°C vs hours).

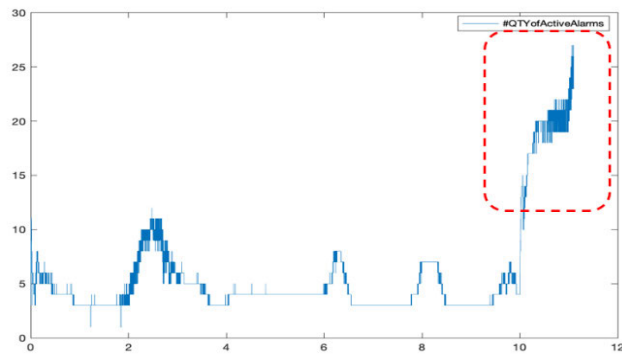**FIGURE 16.** Purge rate (kscmh vs hours).

FIGURE 17. Trend of active alarms timeline (hours).

path to trip in this scenario, and the first path is the reactor's high temperature and high pressure, which lead to the Trip to protect the reactor: *TAH-13 -> TAH-09 -> TAHH-11 -> PAH-01 -> PAHH-02 -> Trip*.

The second path was the high-pressure path in the feedback line on the stripper, which caused the Trip to protect the stripper. *TAH-23 -> PAH-07 -> TAHH-25 -> PAHH-08 -> Trip*.

The third path shows the reactor's high-pressure path, which caused overfilling and high-pressure of the
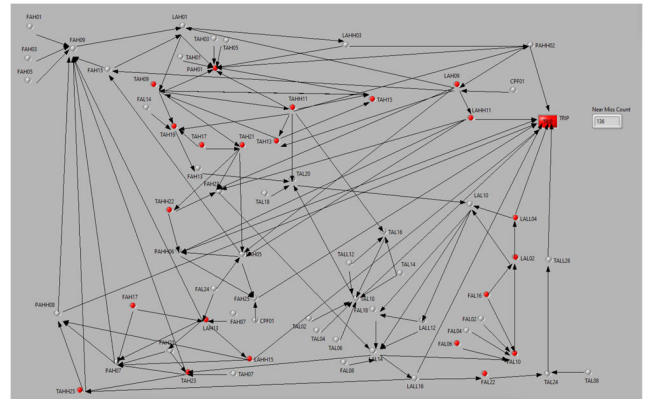
FIGURE 18. AGM screenshot at the very last seconds.

downstream equipment, e.g., condenser and separator and high purge to the Trip. *PAH-01 -> LAH-09 -> PAH-05 -> LAHH-11 -> PAHH-06 -> FAH-25 -> Trip*.

The fourth path is related to the cooling water system high temperature in the separator leads to increased pressure: *TAH-19 -> TAH-21 -> PAH-05 -> LAHH-11 -> PAHH-06 -> Trip*.

The fifth path indicates a different pattern in response to the high pressure. The feed flow was reduced, which consequently reduced the level in the feedback loop (stripper) to avoid damage to the stripper trip alarm was activated. *FAL-06 -> FAL-10 -> LAL-02 -> LALL-04 -> Trip*.

The previously mentioned appointments display a distinct pattern of unusual event progression in this study, providing the operator with valuable information to promptly respond and prevent trip activation.

C. MANIPULATING THE FEED PID CONTROLLER

In this scenario, we attempted to cause operational issues by destabilizing the feed flow controllers by manipulating the proportional factors of the PID controllers. Additionally, to increase the steady-state error of the PID controllers by manipulating the integrator factor. This allowed us to observe the abnormal event progression pattern and confirm the alarm system's effectiveness; the changes are detailed in Table 5.

TABLE 5. PID parameters manipulation.

Feed	Original I-Factor	Manipulated I-Factor	Original Kc	Manipulated Kc
A Feed	0.001/60	0.001/600	0.01	0.3
D Feed	0.001/60	0.001/600	1.06E-06	1.60E-03
E Feed	0.001/60	0.001/600	1.80E-06	1.80E-02
A&C Feed	0.001/60	0.001/600	0.003	0.2

The consequences of the feed flow becoming noisy for this process are evident in Figures 19 and 20. Figure 21 shows that the reactor temperature rose and caused a surge in pressure, leading to the trip. Despite the controllers' attempts to lower
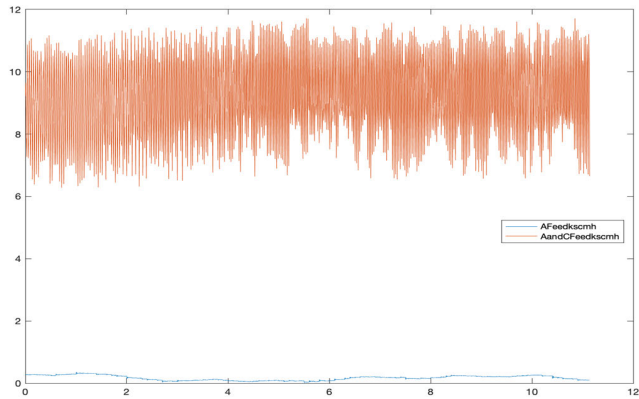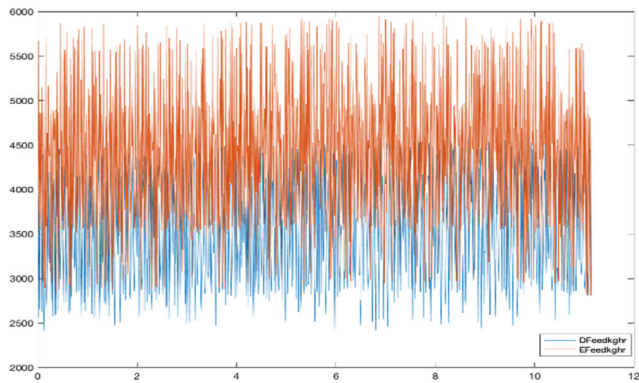
FIGURE 19. A and A&C feed flow (kscmh vs hours).
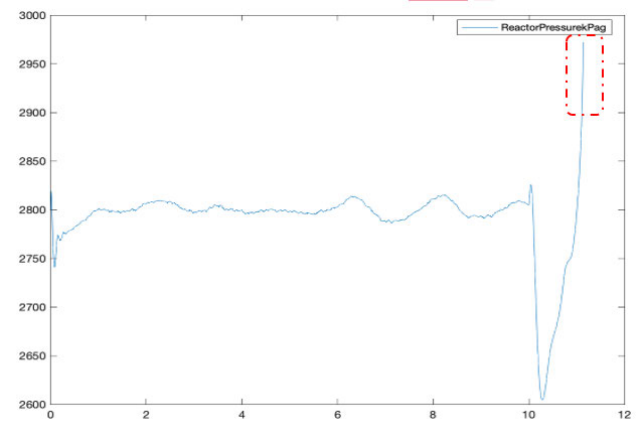

FIGURE 20. D and E feed flow (kg/hr vs hours).
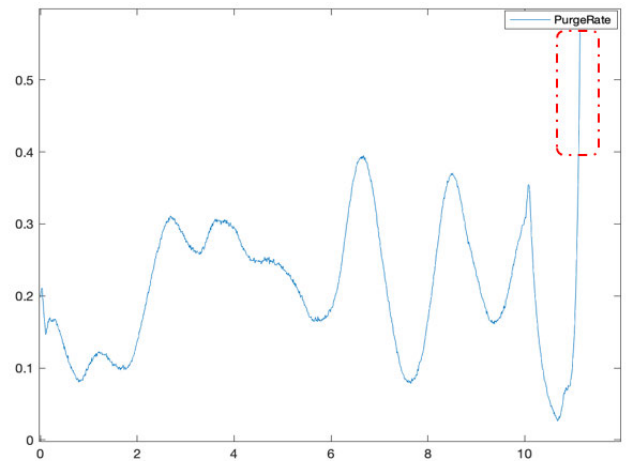

FIGURE 21. Reactor pressure.

FIGURE 22. Purge rate.

FIGURE 23. Production, quality and operation cost.

FIGURE 24. Trend of the active alarms.

the reactor level and subsequently reduce pressure and temperature, it proved to be inadequate. Figure 22 demonstrates that the increased reactor pressure resulted in downstream equipment experiencing high pressure and high purge.

After reviewing the concerning trend shown in Figure 24, there were multiple instances of alarm flooding. However, it is important to note that the number of activated alarms peaked at 30 after the tenth hour of operation before the process eventually tripped.
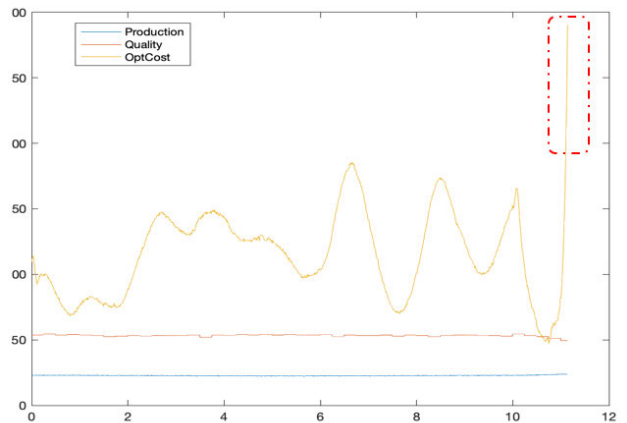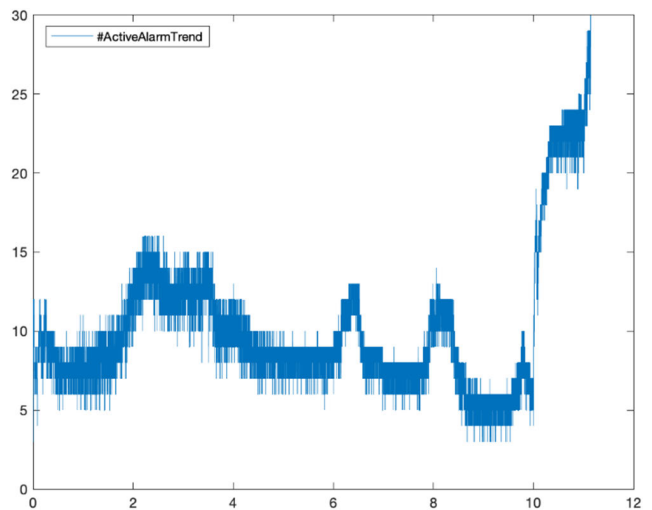
The first path is related to the low feed into the reactor, which caused the low-low level that may cause damage to the catalyst or reactor, so the trip was triggered.
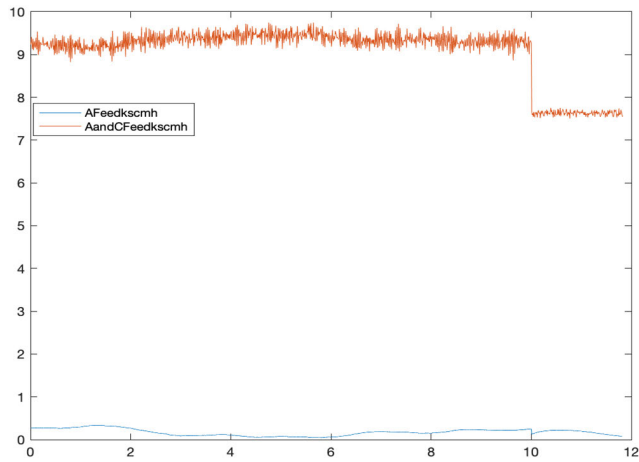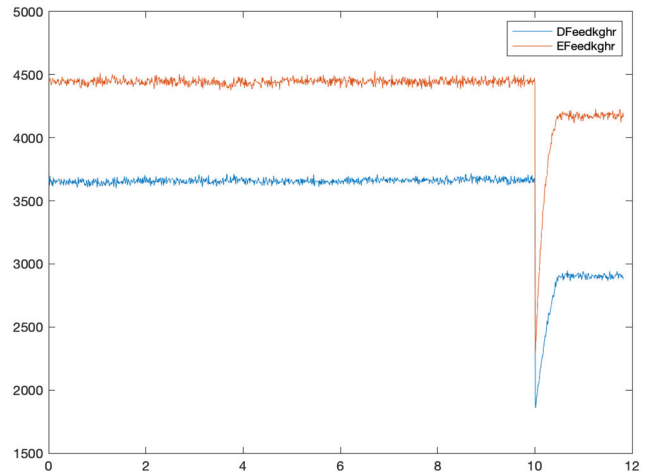
FIGURE 25. A and A+C feed.

FIGURE 26. D and E feed.

Therefore, operators should be able to address the issue by tracking this path. FAL-04&05 -> FAL-10 -> LAL-02 -> LALL-04 -> Trip.

The second path shows the high-temperature path, which was the first path that triggered the trip. Reducing the cooling water caused the reactor high-high temperature, which progressed through downstream equipment. As the cooling water on the condenser decreased, the process fluid with high temperature transferred to the separator, which can damage the separator and increase the purge rate so, initiating the trip: TAH-15 -> TAH-09 -> TAHH-11 -> TAH-19 -> TAH-21-> TAH-22 -> Trip.

The third shows the high level on the stripper, which with the boiler on, can cause increased pressure and blow out: FAH-07 -> LAH-13 -> LAHH-15 -> Trip.

The fourth path was the last abnormal event progression. Due to the high temperature inside the reactor, the controllers reduced the feed flows and the low-level path formed and ended in the trip. FAL-10 -> LAL-02 -> LALL-04 -> Trip.

D. REDUCED FEED RATE
Up until now, we have mainly examined high process values linked to abnormal situations. However, we will now focus on abnormal situations related to low process values. To simulate this scenario, we will decrease the feed rate to 50% of the normal rate using feed valves V-1001, V-1002, V-1003, and V-1004 after 10 hours of operation. Our goal is to observe the low/low-low alarms activate during the process. Refer to Figures 25 and 26 to see how the feed flow decreases to 50% after 10 hours of operation. Figures 27 and 28 show that the reactor process variables are mainly in the normal range, and only the reactor level reduced as expected.

At 11:49:20, following the onset of the abnormal situation, a considerable number of alarms were triggered, reaching a total of 21 as displayed in Figure 28. Subsequently utilizing the activated APTTs, AGM was able to determine the underlying cause and progression of the failure successfully. Based on the analysis of the active APTTs shown
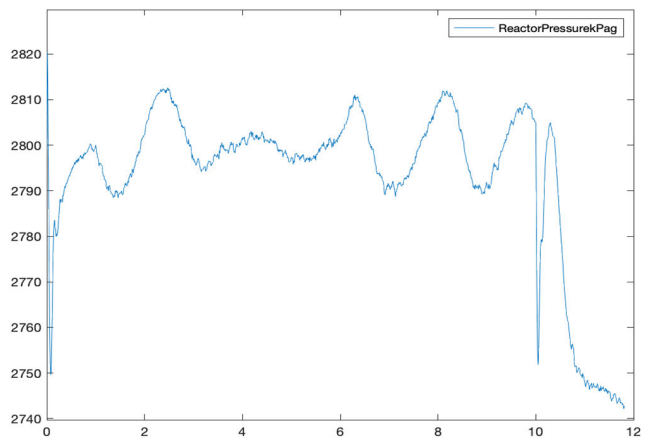

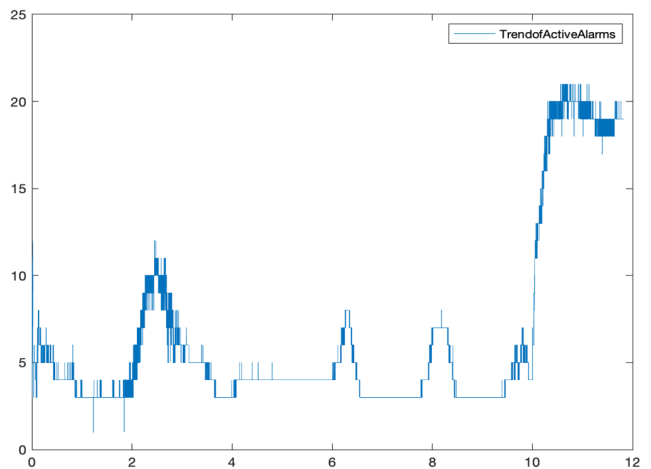**FIGURE 27.** Reactor pressure.

FIGURE 28. Active alarm trend.

in Figures 29 and 30, it has been established that there are four main routes of alarm activation progression associated with the low level of the primary equipment. The initial path is related to the reactor, where a decrease in feed flows
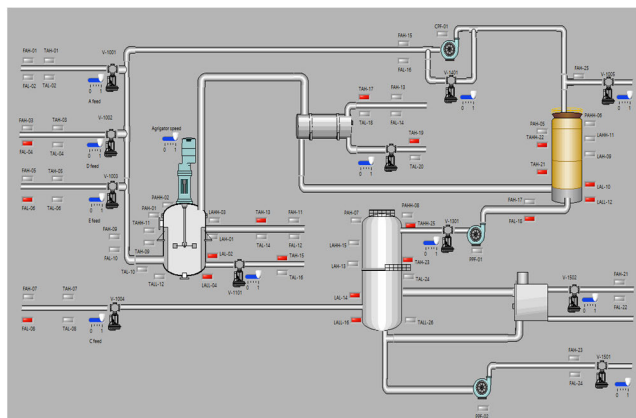
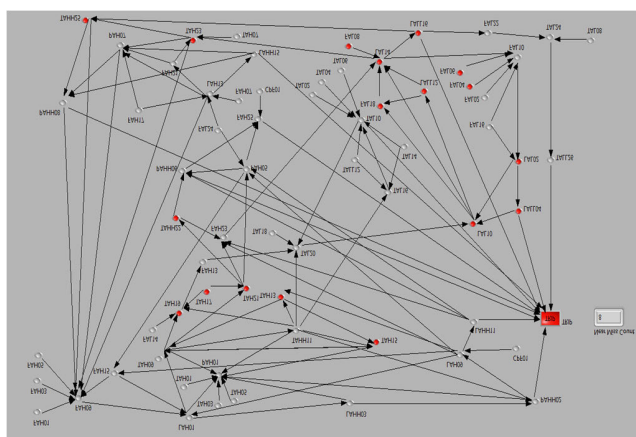**FIGURE 29.** The HMI screenshot (Last seconds to trip).

FIGURE 30. AGM screenshot at the very last seconds.

resulted in a drop in the level inside the reactor. A trip was triggered to avoid any damage to the catalyst or equipment: FAL-02, 04, &06 -> LAL-02 -> LALL-04 ->Trip. The second issue pertains to the stripper's low level, which has the potential to harm high-temperature equipment while the boiler is in operation: FAL-08 & FAL-18 -> LAL-14 -> LALL-16 -> Trip. In the third path, the stripper is affected by the high-temperature alarm that had escalated due to the boiler. This caused the trip initiation after the high-high temperature alarms were triggered.TAH-09 -> TAH-19 -> TAH-21 -> TAH-23 -> TAHH-25 -> Trip. The fourth path concerns the feedback loop from the low separator level. This caused low flow to the stripper, resulting in low flow inside the reactor, ultimately leading to a trip.FAL-08 -> LAL-14 -> LALL-16 -> TAH-25 -> FAL-18 -> LAL-10 -> LALL-12 -> Trip.

IV. CONCLUSION

Designing and implementing an effective alarm system remains a common challenge in modern industrial plants. A key difficulty in this process is properly tuning the alarm setpoints, which can result in alarm flooding or nuisance alarms. This study employs the newly developed alarm

graph modelling (AGM) approach to address this challenge, enhance alarm setpoint tuning, and justify alarm implementation. The approach's first stage involves designing and implementing the TEP's alarm system, which is employed similarly to the actual process operation where the process is supervised in different layers for the supervisory control in the LabView environment via Modbus data communication, then the process operated for hundred hours of simulation to review the alarm tuning according to the AGM. Next, the verification process assesses the alarm activation sequence in four failure scenarios, ensuring that it aligns with abnormal process variables. The AGM captures all alarm activation paths to failure, including failures in the process operation, such as noisy controllers, valve PID controllers with steady-state error, reduced coolant, and reduced feed.

Comparing the AGM approach with the scenarios reveals that it is more effective in identifying abnormal events and addressing failed or poorly commissioned alarms. The AGM provides significant benefits to operators and engineers, such as identifying root causes and capturing inconsistencies in alarm design compared to other approaches, which require massive datasets as described in [6] and [11]. Additionally, the AGM's real-time capabilities make it particularly advantageous for commissioning purposes. Overall, the AGM approach offers a valuable solution to the challenges associated with designing and implementing industrial alarm systems. Its effectiveness in identifying and addressing issues makes it a worthwhile investment for any industrial plant seeking to improve the alarm system. In the upcoming phase of this series, studies on alarm issues are scheduled to take place, as the alarm system has demonstrated potential for further investigations. Although it is important to note that the simulation does have its limitations, such as memory saturation and communication failure, progress is being made towards addressing these issues.

REFERENCES

[1] D. H. Rothenberg, *Alarm Management for Process Control: A Best-Practice Guide for Design, Implementation, and Use of Industrial Alarm Systems*. New York, NY, USA: Momentum Press, 2009.

[2] S. S. Niu and D. Xiao, "Process control overview," in *Process Control: Engineering Analyses and Best Practices*. Cham, Switzerland: Springer, 2022, pp. 3–23.

[3] K. Parsa and M. Hassall, "An enhanced advisory system to improve situational awareness and abnormal situation management," in *Proc. Annu. IEEE Int. Syst. Conf. (SysCon)*, Apr. 2018, pp. 1–6.

[4] S. R. Kondaveeti, I. Izadi, S. L. Shah, T. Black, and T. Chen, "Graphical tools for routine assessment of industrial alarm systems," *Comput. Chem. Eng.*, vol. 46, pp. 39–47, Nov. 2012.

[5] M. S. Afzal, T. Chen, A. Bandehkhoda, and I. Izadi, "Performance assessment of time-deadbands," in *Proc. Amer. Control Conf. (ACC)*, May 2017, pp. 4815–4820.

[6] K. Parsa, M. Hassall, and M. Naderpour, "Process alarm modeling using graph theory: Alarm design review and rationalization," *IEEE Syst. J.*, vol. 15, no. 2, pp. 2257–2268, Jun. 2021, doi: 10.1109/JSYST.2020.3019041.

[7] M. Naderpour, J. Lu, and G. Zhang, "An intelligent situation awareness support system for safety-critical environments," *Decis. Support Syst.*, vol. 59, pp. 325–340, Mar. 2014.

[8] T. Niyazmand and I. Izadi, "Pattern mining in alarm flood sequences using a modified PrefixSpan algorithm," *ISA Trans.*, vol. 90, pp. 287–293, Jul. 2019.

[9] J. C. Laberge, P. Bullemer, M. Tolsma, and D. V. C. Reising, "Addressing alarm flood situations in the process industries through alarm summary display design and alarm response strategy," *Int. J. Ind. Ergonom.*, vol. 44, no. 3, pp. 395–406, May 2014.

[10] S. Charbonnier, N. Bouchair, and P. Gayet, "Fault template extraction to assist operators during industrial alarm floods," *Eng. Appl. Artif. Intell.*, vol. 50, pp. 32–44, Apr. 2016.

[11] K. Parsa, M. Hassall, and M. Naderpour, "Enhancing alarm prioritization in the alarm management lifecycle," *IEEE Access*, vol. 10, pp. 99–111, 2022.

[12] J. J. Downs and E. F. Vogel, "A plant-wide industrial process control problem," *Comput. Chem. Eng.*, vol. 17, no. 3, pp. 245–255, Mar. 1993.

[13] S. Yin, S. X. Ding, A. Haghani, H. Hao, and P. Zhang, "A comparison study of basic data-driven fault diagnosis and process monitoring methods on the benchmark Tennessee eastman process," *J. Process Control*, vol. 22, no. 9, pp. 1567–1581, Oct. 2012.

[14] A. Bathelt, N. L. Ricker, and M. Jelali, "Revision of the Tennessee eastman process model," *IFAC-PapersOnLine*, vol. 48, no. 8, pp. 309–314, 2015.

[15] L. T. Antelo, J. R. Banga, and A. A. Alonso, "Hierarchical design of decentralized control structures for the Tennessee eastman process," *Comput. Chem. Eng.*, vol. 32, no. 9, pp. 1995–2015, Sep. 2008.

[16] N. L. Ricker, "Optimal steady-state operation of the Tennessee eastman challenge process," *Comput. Chem. Eng.*, vol. 19, no. 9, pp. 949–959, Sep. 1995.

[17] N. L. Ricker, "Decentralized control of the Tennessee eastman challenge process," *J. Process Control*, vol. 6, no. 4, pp. 205–221, Aug. 1996.

[18] P. Ponce-Cruz, A. M. Gutiérrez, R. A. Ramírez-Mendoza, E. M. Flores, A. A. O. Espinoza, and D. C. B. Silva, "*A Practical Approach to Metaheuristics Using LabVIEW and MATLAB*. Boca Raton, FL, USA: CRC Press, 2020.

[19] R. Jennings and F. De La Cueva, *LabVIEW Graphical Programming*. New York, NY, USA: McGraw-Hill, 2020.

[20] *Human Machine Interfaces for Process Automation Systems*, Standard ANSI/ISA-101.01-2015, American National Standard, Jul. 2015.

MAUREEN HASSALL is currently the Director of the Industrial Safety and Health Centre, Sustainable Minerals Institute, The University of Queensland. Her expertise crosses the fields of industrial risk management, systems safety engineering, and human factors. She works collaboratively with industry professionals to develop better human-centered risk management and safety engineering approaches that improve companies' oper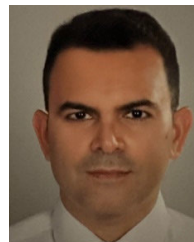ational performance and competitiveness. She also develops and delivers process safety, systems safety engineering, risk management, and human factors training, education, and expert advice to students and industry. Her industry-focused research is motivated by 18 years of industry experience working in a number of different countries and a variety of roles including specialist engineering.

MOHSEN NADERPOUR is currently a Senior Risk Advisor with Transport for NSW and an Industry Fellow with the Australian Artificial Intelligence Institute (AAII), University of Technology Sydney (UTS). He began the career as a safety professional in high-risk industries, including transportation and oil, before taking up a position in academia as a Research Fellow with the Global Big Data Technologies Centre, U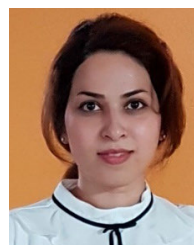TS, and then a Lecturer and a Senior Lecturer with the Faculty of Engineering and IT. His research interests include applied artificial intelligence, risk engineering, computational intelligence, and decision-making.

MOBIN POURREZA received the bachelor's degree in electronic engineering and the M.E. degree from the K. N. Toosi University of Technology (KNTU), Tehran, Iran, in 2005. He is currently pursuing the master's degree in embedded system engineering with Fachhochschule Dortmund, Dortmund, Germany. He has a sound background in electronic circuit design, power transformers and switchgear, distribution systems and automation, and control system programming.

KOUROSH PARSA (Senior Member, IEEE) received the B.Sc. degree in electrical engineering-control systems and the M.Sc. and Ph.D. degrees in systems engineering from The University of Queensland (UQ). He works across various industries, such as oil and gas, refineries, LNG, and rails. He has gained extensive experience in qualitative and quantitative reliability analysis, safety cases, RAMS, HAZOP, FMEA, LOPA, SIL study, systems and software safety, and OT cybersecurity. He also has a background in data science, big-data management, deep learning, modeling and simulation, RCA, and incident investigation.

FAHIMEH RAMEZANI is currently a Senior Lecturer with the School of Computer Science, University of Technology Sydney (UTS), Sydney, Australia. In addition, she is a Core Member of the Artificial Intelligence Institute (AAII). Before joining UTS, she had seven years of industry experience as a Software Developer and a Researcher in different domains. Her research interests include cloud/fog computing, optimization, and artificial intelligence.

• • •